

TABLE I  
COMPARISON OF COUPLED LINE PARAMETERS OF NONIDENTICAL  
LINE MICROSTRIP COUPLER

$\epsilon_r$	$\epsilon_r/\epsilon_0 = 1.0$	TRIPATHI and CHANG								This Method						
		S/H	$W_2/W_1$	$Z_{01}$	$Z_{01}$	$Z_{02}$	$Z_{02}$	$V_{01} \times 10^3$	$V_{02} \times 10^3$							
6.0	0.4	3.0	87	50	37.68	21.66	1.39	1.55	91.6	52.68	36.33	20.89	1.365	1.54		
10.0	0.2	3.0	71	38	28.9	15.46	1.07	1.26	72.93	39.19	29.63	15.92	1.079	1.292		
	0.6	2.0	60	41	36.95	25.75	1.08	1.22	62.58	41.41	37.33	24.7	1.087	1.246		
	0.6	2.6	61.5	42.5	30.39	21.83	1.07	1.21	63.45	42.38	30.77	20.56	1.073	1.209		
	0.6	3.0	62.5	43.5	26.94	18.75	1.059	1.21	63.76	42.88	27.59	18.56	1.053	1.205		
	1.0	2.0	56.5	43.0	34.8	26.48	1.075	1.22	57.5	44.1	35.35	27.12	1.085	1.19		
	1.0	3.0	58.0	46.0	26.4	20.93	1.07	1.20	58.9	45.2	26.43	20.27	1.056	1.18		
14.0	0.4	3.0	55.0	35.0	24.45	15.56	0.88	1.05	55.5	35.05	24.15	15.23	0.898	1.051		
16.0	0.4	3.0	50.0	32.0	22.23	14.22	0.80	1.00	51.44	32.87	22.59	14.43	0.897	0.988		

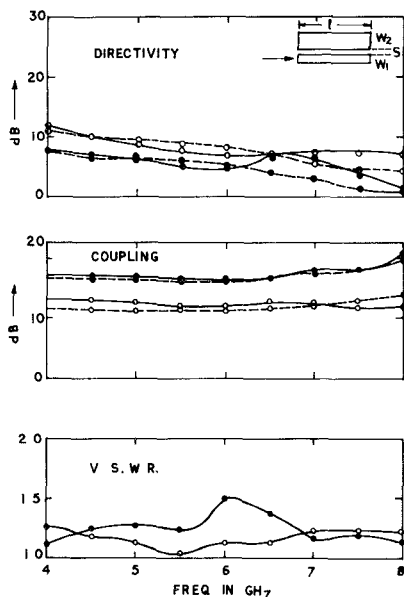


Fig. 3. Experimental and theoretical performance of two nonidentical line microstrip couplers. Coupler A —○—  $W_1/H = 0.945$ ,  $W_2/H = 1.89$ ,  $S/H = 0.315$ . Coupler B —●—  $W_1/H = 0.945$ ,  $W_2/H = 1.89$ ,  $S/H = 0.819$ . Experiment —. Theory ----.

tric constant of the substrate ( $\epsilon_r$ ) for a given asymmetry. As expected, there is a significant variation in mode velocities with  $\epsilon_r$ . The computed values of mode impedances and normal-mode velocities for different  $S/H$ ,  $W_2/W_1$ , and  $\epsilon_r$  values are compared in Table I with those of Tripathi and Chang [2]. The values of the parameters obtained from the two methods are quite close (within 5 percent). However, for the case of tight coupling ( $S/H < 0.2$ ), the agreement is rather poor.

### III. EXPERIMENTAL RESULTS AND DISCUSSION

Two nonidentical couplers of 11- and 16-dB coupling at the center frequency of 5.5 GHz have been designed on 25-mil-thick ( $H$ ) alumina substrate ( $\epsilon_r = 9.6$ ). The length of the coupled region  $L$  has been chosen such that at the center frequency  $(\beta_c + \beta_\pi)/2 = \pi/2$ . At 5.5 GHz,  $l$  turns out to be 0.544 cm. The ratio of auxiliary linewidth to main linewidth for both the couplers is 2, and the input is applied to the main line of smaller width ( $W/H = 0.945$ ). The performance of the couplers was measured in the frequency range 4–8 GHz using an HP 8755 coax reflectometer system, and the results are given in Fig. 3 (solid line). Theoretical calculations of coupling and directivity

using the relations (1)–(7) in the same frequency range are shown in the same figure (dotted line). A comparison of experimental and theoretical results of coupling and directivity of the two nonidentical line couplers shows a close agreement around the center frequency.

### IV. CONCLUSIONS

A method of computing normal-mode parameters using the empirical relations of coupling coefficients of nonidentical coupled lines has been presented. The computed values have been compared with Tripathi and Chang. The agreement between theoretical and experimental performance of two couplers made on alumina substrate is found to be good. The principal limitations of the method are that this is applicable for loose coupling ( $S/H < 0.2$ ) and for substrates having values of relative dielectric constant greater than 6.

### ACKNOWLEDGMENT

The authors wish to thank the reviewers for useful suggestions.

### REFERENCES

- [1] R. A. Speciale and V. K. Tripathi, "Wave modes and parameter matrices of non-symmetrical coupled lines in a non-homogeneous medium," *Int. J. Electron.*, vol. 40, no. 4, pp. 371–375, 1976.
- [2] V. K. Tripathi and C. L. Chang, "Quasi-TEM parameters of non-symmetrical coupled microstrip lines," *Int. J. Electron.*, vol. 45, no. 2, pp. 215–223, 1978.
- [3] J. L. Allen, "Non-symmetrical coupled lines in an inhomogeneous dielectric medium," *Int. J. Electron.*, vol. 38, pp. 337–347, Mar. 1975.
- [4] H. G. Bergandt and R. Pregla, "Calculation of the even- and odd-mode capacitance parameters of coupled microstrips," *Arch. Elek. Übertragung*, vol. 26, pp. 153–158, 1972.
- [5] G. Kowalski and R. Pregla, "Calculation of the distributed capacitances of the coupled microstrips using a variational integral," *Arch. Elek. Übertragung*, vol. 27, pp. 51–52, 1973.
- [6] T. A. Milligan, "Dimensions of coupled lines and interdigital structures," *IEEE Trans. Microwave Theory Tech.*, vol. MTT-25, pp. 405–410, May 1972.
- [7] S. Kal, D. Bhattacharya, and N. B. Chakraborti, "Empirical relations for capacitive and inductive coupling coefficients of coupled microstrip lines," *IEEE Trans. Microwave Theory Tech.*, vol. MTT-29, pp. 386–388, Apr. 1981.
- [8] V. K. Tripathi, "Asymmetric coupled transmission lines in an inhomogeneous medium," *IEEE Trans. Microwave Theory Tech.*, vol. MTT-23, pp. 734–739, Sept. 1975.
- [9] E. G. Cristal, "Coupled transmission line directional couplers with coupled lines of unequal characteristics impedances," *IEEE Trans. Microwave Theory Tech.*, vol. MTT-14, pp. 333–346, 1966.
- [10] R. A. Speciale, "Even- and odd-mode waves for nonsymmetrical coupled lines in nonhomogeneous media," *IEEE Trans. Microwave Theory Tech.*, vol. MTT-23, pp. 897–908, Nov. 1975.
- [11] M. K. Krage and G. I. Haddad, "Characteristics of coupled microstrip transmission lines—I: Coupled mode formulation of inhomogeneous lines," *IEEE Trans. Microwave Theory Tech.*, vol. MTT-18, pp. 217–222, Apr. 1970.

### An Analysis of a Width-Modulated Microstrip Periodic Structure

N. V. NAIR AND A. K. MALLICK

**Abstract** — The wave propagation along a microstripline with sinusoidally varying width has been investigated. The analysis employs the circuit theory of uniform microstriplines and their step junctions. The wave

Manuscript received May 27, 1983; revised October 7, 1983.

N. V. Nair is with the Department of Electronics and Communication Engineering, College of Engineering, Trivandrum—695016, India.

A. K. Mallick is with the Department of Electronics and Electrical Communication Engineering, Indian Institute of Technology, Kharagpur—721 302, India.

amplitude transmission (WAT) matrix has been successfully used to determine the propagation constant, characteristic impedance, and the input impedance of the terminated line. Samples have been fabricated for the experimental verification of the above-mentioned quantities. Theory and experiment show good agreement.

The filter-like propagation characteristic of the structure is exploited in the realization of a bandstop filter. A graphical design of such a filter is presented and the insertion-loss measurement shows encouraging results.

## I. INTRODUCTION

The development of microstriplines, both uniform and nonuniform, has received greater attention in recent years owing to their practicability at microwave frequencies. Nonuniform transmission lines have been studied and their applications as filters, directional couplers, delay lines, and impedance matching networks have been reported in the past by many authors [1]–[9]. The periodic microstripline may be constructed by modulating its width as a periodic function of length. Such a line can be realized by sinusoidally varying the width or by sinusoidally varying the characteristic impedance level. In this paper, the analysis of sinusoidal width modulation is presented. The latter case of impedance modulation will be reported soon in another paper.

The distributed loading is physically achieved in this problem by varying the width cosinusoidally along the direction of propagation. The circuit theoretical approach using the wave amplitude transmission (WAT) matrix has been employed to study the propagation properties of the structure. The analysis is simpler than the field theoretical approach and takes less time for computation. The accuracy of the technique can, in principle, be improved to any degree at the cost of computational time. The disadvantage of the matrix method is that the closed-form expressions may not be feasible if accuracy is at premium.

Fig. 1 shows the periodic line under consideration. The analysis establishes the functional behavior of the periodic line with respect to the propagation constant, the phase and group velocities, the characteristic impedance, and the input impedance. It employs the WAT matrix of elementary sections consisting of uniform lines and their step junctions. Stepped-width approximation of the sinusoidally modulated line is considered. Expressions have been developed for the propagation constant and characteristic impedance of the line and also the input impedance when the line is terminated. Computer-aided analysis has been used for higher orders of approximation where the closed-form expressions are extremely difficult to obtain. Experiments have been carried out and show good agreement with the theory.

Finally, a graphical method for the design of a bandstop filter is reported. It is a direct application of the analysis carried out and the results obtained. The filter is easy to design and shows a sharp rejection band. It finds many applications in the field of modern electromagnetic management. The depth of modulation and the periodicity are the two parameters which control the characteristics of the filter.

The structure has also been utilized in the design of a bandpass filter which shows a null of about 75 dB. This may find potential use in the up-link of a Satellite Communication system. The structure can also be used as a patch radiator, for broad-banding in the design of directional couplers, etc. These applications are not reported here.

## II. THEORETICAL ANALYSIS

### A. Propagation Constant

Fig. 1 illustrates the sinusoidally varying microstripline with mean width  $W_0$  and periodicity  $p$ . The continuously modulated strip width is approximated as a cascaded combination of a

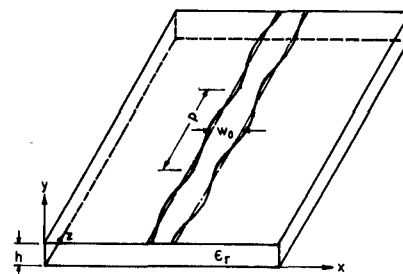


Fig. 1. Microstrip with sinusoidally varying width.

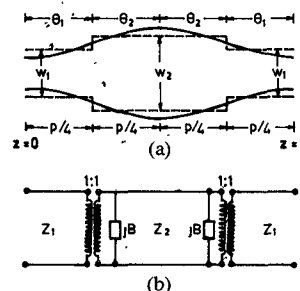


Fig. 2. (a) First-order approximated unit element. (b) Its equivalent circuit.

number of elementary uniform sections of different widths, as shown in Fig. 2 for the first-order approximation. The analysis then uses the WAT matrix [10], [11] of each such section and the line junctions to construct the overall WAT matrix of a unit element of period  $p$ . The stepped-width approximation is shown in Fig. 2(a), while Fig. 2(b) indicates the electrical equivalent circuit of the approximated unit cell. It is shown that the resulting configuration consists of three uniform lines with their junctions, of widths  $W_1$  and  $W_2$  and impedances  $Z_1$  and  $Z_2$ . The excess charge at the junctions presents capacitive susceptance  $B$  [12]–[14]. The change in impedance level at the junctions is accounted for by considering an ideal transformer with a  $1:k$  ratio. For small step sizes, the turn ratio  $k$  equals unity.

In Fig. 2, the modulated line with periodicity  $p$  is divided into four equal sections of length  $p/4$  and widths  $W_1 = W_0(1 - 0.5m)$  and  $W_2 = W_0(1 + 0.5m)$ , where  $m$  is the modulation index. Using the parameters of the overall WAT matrix, the propagation constant  $\gamma$  can be obtained [10] as

$$\begin{aligned} \cosh(\gamma p) = & \cos 2\theta_1 \cos 2\theta_2 \\ & - (1/2K_1)(1 + K_1^2 - B^2 Z_1^2) \sin 2\theta_1 \sin 2\theta_2 \\ & - BZ_2(K_1 \sin 2\theta_1 \cos 2\theta_2 + \cos 2\theta_1 \sin 2\theta_2) \end{aligned} \quad (1)$$

where  $K_1 (= Z_1/Z_2)$  is the ratio of the characteristic impedances of the microstriplines with widths  $W_1$  and  $W_2$  and electrical lengths  $\theta_1$  and  $\theta_2$ .  $Z_n$  ( $n = 1, 2$ ) is the characteristic impedance of uniform microstriplines as given by Wheeler [15]. For all practical microstrip steps considered here, the shunt capacitive contribution is found to be quite small, and so is neglected. Thus, for the lossless case,  $\beta p$  may be obtained as

$$\beta p = \cos^{-1} [\cos 2\theta_1 \cdot \cos 2\theta_2 - (1/2K_1)(1 + K_1^2) \sin 2\theta_1 \sin 2\theta_2]. \quad (2)$$

The effect of the inhomogeneous dielectric of microstrip is accounted for by using the effective dielectric constant  $\epsilon_{\text{eff}}$  [16].

The composition of Fig. 2 may be further extended to approximations of second order, third order, and so on, each time increasing the number of steps by two. The widths of the approximated uniform lines may be determined from the following

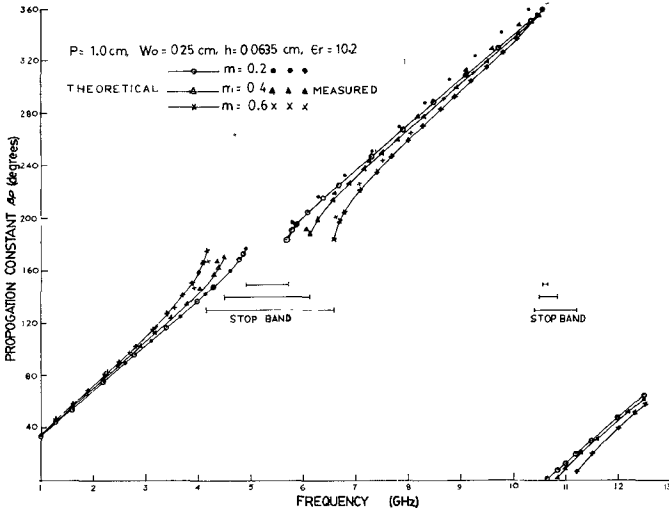


Fig. 3. Propagation characteristic.

equation:

$$W_n = W_0 \left[ 1 - m \cos \frac{(2n-1)\pi}{2(N+1)} \cdot \cos \frac{\pi}{2(N+1)} \right] \quad (3)$$

where  $N$  is the order of approximation and  $n$  is an integer,  $1, 2, \dots, (N+1)$ . For the second-order approximation

$$\begin{aligned} \beta p = & \cos^{-1} \left[ (-1/8K_1K_2) \{ (1+K_1^2)(1+K_2^2) \sin 2\theta_1 \cos 2\theta_2 \right. \\ & + 4K_1(1+K_2^2) \cos 2\theta_1 \sin 2\theta_2 \} \sin 2\theta_3 + \{ (1-K_1^2) \right. \\ & \cdot (1-K_2^2) + 4K_2(1-K_1)^2 \cos 2\theta_3 \} \sin 2\theta_1 \sin 2\theta_2 \} \end{aligned} \quad (4)$$

where  $K_1 = Z_1/Z_2$  and  $K_2 = Z_2/Z_3$ . Improved accuracy is achieved by using computer-aided analysis. All the theoretical data given in this paper are computed to fourth decimal place accuracy using  $N = 8$ .

The phase characteristic of Fig. 3 shows the presence of alternate passbands and stopbands. Their occurrence is related to the physical conditions determined by  $|\cos(\beta p)|$ . The position and the width of the stopbands can be related to the physical parameters of the structure using design curves as shown in Section III.

### B. Characteristic Impedance

Characteristic impedance is defined for an infinitely long periodic line, as the impedance offered to the voltage or current waves at the input terminals of a periodic cell [10]. The normalized impedance is derived in terms of the elements of the overall WAT matrix as

$$Z_0 = \frac{2A_{12} - A_{11} + A_{22} \pm [(A_{11} + A_{22})^2 - 4]^{1/2}}{2A_{12} + A_{11} - A_{22} \mp [(A_{11} + A_{22})^2 - 4]^{1/2}}. \quad (5)$$

Its variation with frequency is plotted in Fig. 4. It is seen that there are two stopbands in the range 1 to 12.5 GHz. The dominant one is centered around 5.3 GHz and the other at 10.6 GHz. The width of the stopband depends very much on the value of  $m$  and it increases with  $m$ , which is also evident in Fig. 3. It is further observed that the characteristic impedance is real and close to unity in the passband. Its constancy in the range is satisfactory except in the vicinity of cutoff.

### C. Input Impedance of the Terminated Periodic Line

Consider a periodic line with  $K$  cells, each having a period  $p$ , and terminated in a normalized load  $Z_L$  at the  $K$ th terminal

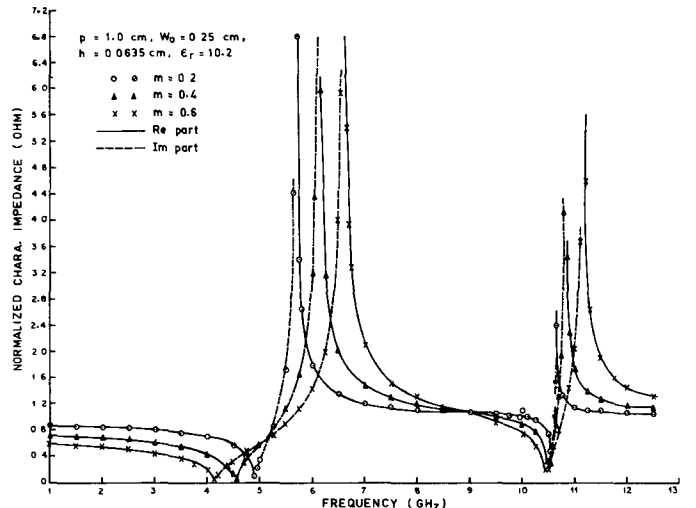


Fig. 4. Characteristic impedance versus frequency.

plane. By knowing the reflection coefficients at the zeroth and  $K$ th terminals, one can determine the input impedance [17], [10]. The expression is derived as

$$Z_{in} = \frac{Z_B^+ Z_B^- [1 - (Z_B^- Z_B^+) (Z_L - Z_B^+) e^{-2j\beta L} / (Z_L - Z_B^-)]}{[Z_B^- Z_B^- (Z_L - Z_B^+) e^{-2j\beta L} / (Z_L - Z_B^-)]} \quad (6)$$

where  $L = Kp$  is the length of the structure, and  $Z_B^+$  and  $Z_B^-$  are Bloch-wave impedances in the  $+z$  and  $-z$  directions, respectively. Since the structure considered is a symmetrical one,  $Z_B^+ = -Z_B^- = Z_0$ . The ambiguity in the sign of  $Z_0$  may be avoided by noting that, in the propagation band, it is always real and positive (see (5)), to be consistent with the choice of positive direction for current. Replacing the Bloch-wave impedances by  $Z_0$  of (5), (6) reduces to a simple expression similar to that of a uniform line. Thus

$$Z_{in} = Z_0 \frac{Z_L + jZ_0 \tan \beta L}{Z_0 + jZ_L \tan \beta L}. \quad (7)$$

The input reflection coefficient has been calculated for a periodic line consisting of eight sections with  $p = 1$  cm. It is shown in Fig. 8, for  $Z_L = 50 \Omega$  and  $40 \Omega$ . The results presented in this figure are discussed in Section V.

### III. REALIZATION OF A BANDSTOP FILTER

The filter-like behavior of the modulated microstrip line is evident from the propagation characteristics of Fig. 3. The structure can be used as a bandstop filter. Since closed-form relations have not been found, it is not possible to design the filter in the conventional way. Therefore, a graphical method has been developed.

As the modulation parameter  $m$  is varied, the average volume per cell is not changed and the positions of the stopbands remain unchanged [18]. Fig. 6 gives the design curves, constructed with the data available from the dispersion curves.  $f_0$  and  $\Delta f$ , respectively, are the center frequency and the width of the stopband.

As an example, consider the design of a bandstop filter with  $f_0 = 5.3$  GHz and  $\Delta f = 1.6$  GHz. Choosing  $W_0 = 0.25$  cm and a substrate with  $\epsilon_r = 10.2$  and  $h = 0.0635$  cm, and using curves of Fig. 6,  $p$  is found to be 1 cm for  $f_0 = 5.3$  GHz. For this  $p$ ,  $m$  is obtained to be 0.4 corresponding to the given  $\Delta f = 1.6$  GHz. We have constructed a periodic line with  $p$  and  $m$  thus obtained. For experimental purposes, we have chosen to use eleven sections. The measured attenuation characteristic of this line, shown in

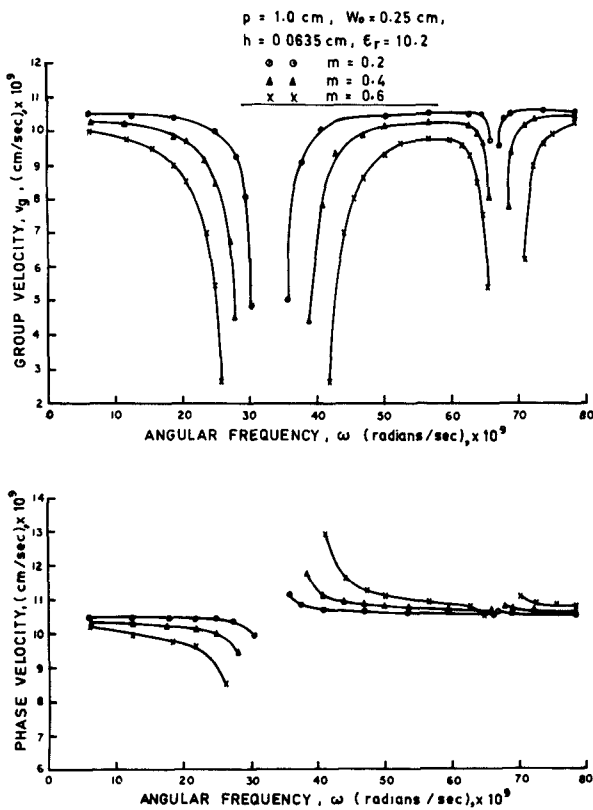


Fig. 5. Phase and group velocities versus frequency.

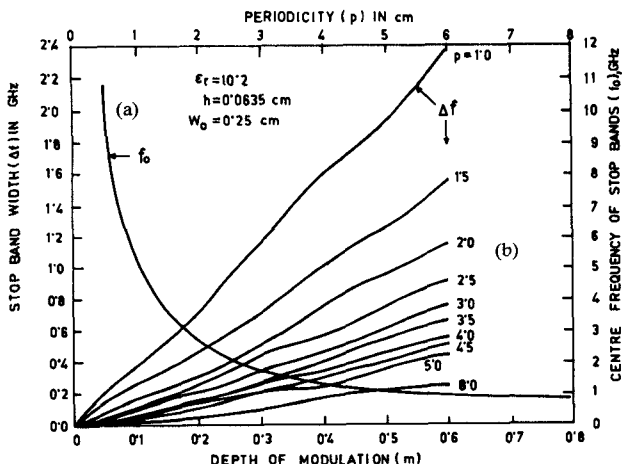
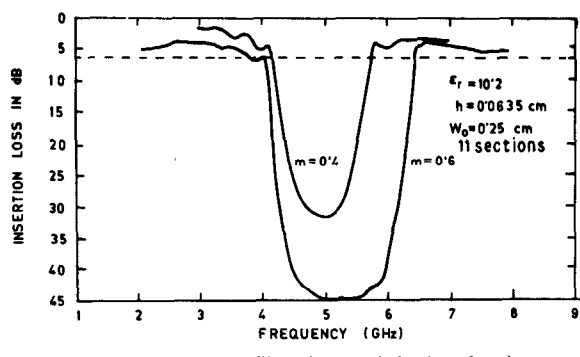
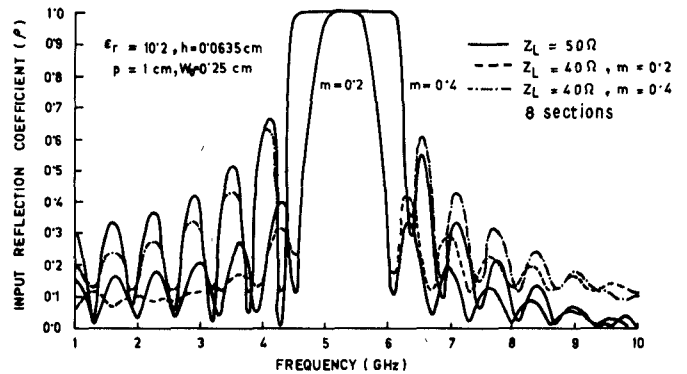
Fig. 6. Filter design curves. (a)  $f_0$  versus  $p$ . (b)  $\Delta f$  versus  $m$ .Fig. 7. Bandstop filter characteristics ( $p = 1$  cm).

Fig. 8. Input reflection coefficient from (7).

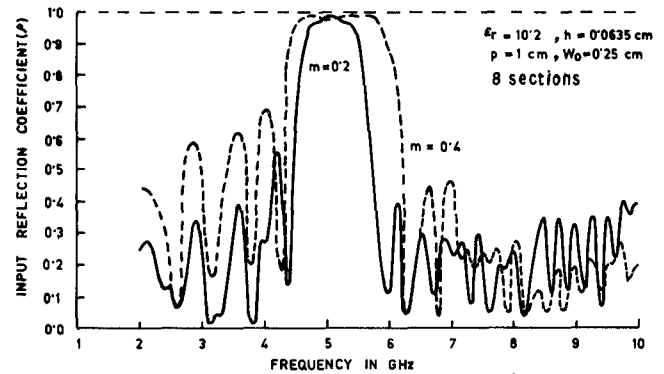
Fig. 9. Input reflection coefficient (measured for  $Z_L = 50 \Omega$ ).

Fig. 7, gives an insertion loss of 33 dB. The insertion loss of the filter may be increased by having higher values of  $m$ . This is also illustrated in the figure for  $m = 0.6$ , where the measured insertion loss is found to be enhanced by 12 dB. A qualitative discussion on the filter characteristics follows in Section V.

#### IV. EXPERIMENTS

The experimental verification of the phase shift per period was accomplished using a Hewlett-Packard Network Analyzer. A number of samples with different  $p$  and  $m$  values were fabricated on a dielectric substrate with  $\epsilon_r = 10.2$  and  $h = 0.0635$  cm. A specific case of  $p = 1$  cm and  $W_0 = 0.25$  cm with three values of  $m$  (0.2, 0.4, and 0.6) is reported here and the phase shift per period as a function of frequency is shown in Fig. 3. In the measurement, the microstrip modulated periodic line with a number of sections (periods) is treated as a resonator by short circuiting at the planes of symmetry such that the images of discontinuities in the shorting planes do not disturb the continuation of the periodic structure in both directions [19]. Under resonance, the input reference plane is at a low impedance level when the output plane is shorted. A tapered section is used at the input end in order to match the impedance of the line to a  $50\Omega$  connector. Initial calibration was done with an identical taper shorted at the line end to fix the input reference plane. The resonant frequencies are noted; the total phase shift at each time is  $n\pi$ , where  $n$  is an integer. The total length of the line should consist of a good number of periods to get sufficient observation points. If the length of the periodic line is eleven periods, for instance, the phase shift per period is  $n\pi/11$ . The value of  $n$  is determined by probing the number of nulls along the resonator. The experimental points are shown in Fig. 3.

Direct measurement of the characteristic impedance is difficult. However, it can be indirectly determined from a knowledge of the input reflection coefficient or, equivalently, the input imped-

ance. The reflection coefficient was measured using a dual directional coupler and a swept amplitude analyzer. Matching of the periodic line was accomplished using a taper. A tapered line of suitable length was used at the input end of an eight-section periodic structure fabricated on a substrate with  $\epsilon_r = 10.2$ . A  $50\Omega$  load was connected at the other end using a microstrip connector. Initial calibration was done with an identical input tapered line which was shorted at the end. Fig. 9 shows the measured input reflection coefficient of the eight-section periodic structure.

The same setup was used for the measurement of insertion loss. It ascertains, as shown in Fig. 7, the frequency characteristics of the bandstop filter. These characteristics are discussed in the following section.

## V. RESULTS AND DISCUSSION

In Fig. 3, the experimental points closely follow the theoretical curves. However, they deviate at the higher frequencies. This may be attributed to the presence of hybrid modes, and dielectric and radiation losses. Also, it can be observed that the stopbands grow wider as  $m$  increases. The phase and group velocities (Fig. 5) are found to be almost constant over a fairly large portion of the passband.

The return-loss measurement shows a moderate amount of ripple in the passband. This is expected from the expression for the input impedance. It may be noted from Fig. 4 that the characteristic impedance is not very sensitive to frequency in the passband, and hence broad-band matching may not be difficult to achieve. The theoretical (Fig. 8) and experimental (Fig. 9) curves of the input reflection coefficient show fairly good agreement. It is also seen in Fig. 8 that with loads lower than  $50\Omega$ , the ripple in the passband is reduced in the frequency range below the stopband and vice versa at frequencies above the stopband. This is also evident in Fig. 4.

The frequency response of the bandstop filter (Fig. 7) shows that its insertion loss increases with  $m$ . A frequency shift away from the theoretically predicted value of  $f_0 = 5.3$  GHz can also be observed in Fig. 7. For  $m = 0.4$ , the measured shift of center frequency is 0.4 GHz, whereas it is only 0.05 GHz for  $m = 0.6$ . At a 6-dB insertion loss, the bandwidths are found to be 1.6 GHz (for  $m = 0.4$ ) and 2.4 GHz (for  $m = 0.6$ ). While the first value agrees exactly with the design data, the second differs by  $+0.05$  GHz from the theoretical value.

## VI. CONCLUSION

An analysis of a sinusoidally modulated microstrip periodic line is given. An experimental investigation has been carried out on lines with several values of  $p$  and  $m$ . In all cases, the experimental results by and large agree with the theory as already discussed. The matching problem has to be improved. This can be achieved to some extent by using substrates of low  $\epsilon_r$ , with  $W_0$  corresponding to  $50\Omega$ . Also, the effect of fabrication tolerance is reduced in this case.

The bandstop filter is very easy to design. Its characteristics can be varied by changing  $p$  and  $m$ . The response has steep skirts. It may perform better than the conventional type of filters.

## REFERENCES

- [1] C. P. Womack, "The use of exponential transmission lines in microwave components," *IRE Trans. Microwave Theory Tech.*, vol. MTT-10, pp. 124-132, Mar. 1962.
- [2] R. N. Ghose, *Microwave Circuit Theory and Analysis*. New York: McGraw-Hill, 1963, ch. 12.
- [3] R. N. Ghose, "Exponential transmission lines as resonators and transformers," *IRE Trans. Microwave Theory Tech.*, vol. MTT-5, pp. 213-217, July 1957.
- [4] H. J. Scott, "The hyperbolic transmission line as a matching section," *Proc. IRE*, vol. 41, pp. 1654-1657, Nov. 1953.
- [5] E. N. Protonotarios and O. Wing, "Analysis and intrinsic properties of the general non-uniform transmission line," *IEEE Trans. Microwave Theory Tech.*, vol. MTT-15, pp. 142-150, Mar. 1967.
- [6] S. Yamamoto, T. Azakami, and K. Itakura, "Coupled non-uniform transmission lines and its applications," *IEEE Trans. Microwave Theory Tech.*, vol. MTT-15, pp. 220-231, Apr. 1967.
- [7] A. K. Sharma and B. Bhat, "Analysis of coupled non-uniform transmission line two-port networks," *Arch. Elek. Übertragung*, vol. 32, pp. 334-337, 1978.
- [8] S. C. Dutta Roy, "Matrix parameters of non-uniform transmission lines," *IEEE Trans. Circuit Theory*, vol. CT-12, pp. 142-143, Mar. 1965.
- [9] M. I. Sobhy and E. A. Hosny, "The design of directional couplers using exponential lines in inhomogeneous media," *IEEE Trans. Microwave Theory Tech.*, vol. MTT-30, pp. 71-76, Jan. 1982.
- [10] R. E. Collin, *Foundations for Microwave Engineering*. New York: McGraw-Hill, 1966, ch. 8.
- [11] A. K. Mallick and G. S. Sanyal, "Electromagnetic wave propagation in a rectangular waveguide with sinusoidally varying width," *IEEE Trans. Microwave Theory Tech.*, vol. MTT-26, pp. 243-249, Apr. 1978.
- [12] P. Benedek and P. Silverster, "Equivalent capacitances for microstrip gaps and steps," *IEEE Trans. Microwave Theory Tech.*, vol. MTT-20, pp. 729-733, Nov. 1972.
- [13] C. Gupta and A. Gopinath, "Equivalent circuit capacitance of microstrip step change in width," *IEEE Trans. Microwave Theory Tech.*, vol. MTT-25, pp. 819-822, Oct. 1977.
- [14] R. Garg and I. J. Bahl, "Microstrip discontinuities," *Int. J. Electron.*, vol. 45, no. 1, pp. 81-87, July 1978.
- [15] H. A. Wheeler, "Transmission line properties of strip on a dielectric sheet on a plane," *IEEE Trans. Microwave Theory Tech.*, vol. MTT-25, pp. 631-647, Aug. 1977.
- [16] M. V. Schneider, "Microstrip lines for microwave integrated circuits," *Bell Syst. Tech. J.*, vol. 48, no. 5, pp. 1421-1444, May 1969.
- [17] J. C. Slater, *Microwave Electronics*. New York: Van Nostrand, 1950, ch. 8.
- [18] M. D. Sirkis, "Application of perturbation theory to the calculation of  $\omega-\beta$  characteristics for periodic structure," *IRE Trans. Microwave Theory Tech.*, pp. 251-252, Mar. 1960.
- [19] D. A. Watkins, *Topics in Electromagnetic Theory*. New York: Wiley, 1958, p. 9.

## Semiconductor Antenna: A New Device in Millimeter- and Submillimeter-Wave Integrated Circuits

F. C. JAIN, MEMBER, IEEE, R. BANSAL, MEMBER, IEEE, AND C. V. VALERIO, JR., MEMBER, IEEE

**Abstract** — A new approach in realizing millimeter- and submillimeter-wave antennas using semiconductor materials is described. The characteristics of these antennas can be controlled during fabrication and/or during operation by modulating the conductivity of the semiconductor. Theoretical computations are presented to evaluate the performance of some typical antenna structures. The physical layout of a monolithic semiconductor antenna with its associated control elements is also described.

## I. INTRODUCTION

Recent advances [1] in the monolithic integrated circuit technology for millimeter-wave systems have provided a new impetus to the design of compatible circuit components. This paper describes a new approach [2] in the realization of millimeter- and

Manuscript received June 15, 1983; revised September 14, 1983.

F. C. Jain and R. Bansal are with the Department of Electrical Engineering and Computer Science, University of Connecticut, Storrs, CT 06268.

C. V. Valerio is with the Phonon Corporation, Simsbury, CT 06070.